

# **3D Underwater Landslide Tsunami Benchmark : laboratory experiments for a smooth rigid slide**

(Based on Enet and Grilli, 2007)

## **1 Introduction**

In the following, we provide background information and details of available data, for a three dimensional (3D) underwater landslide tsunami laboratory benchmark that can be used for validating landslide tsunami models, based on Enet and Grilli's (2007) experiments (Fig. 1).

These experiments were all performed over a plane incline with angle  $\theta = 15^\circ$ , using a smooth streamlined Gaussian-shaped body, released at time  $t = 0$  from a series of initial submergence depths  $d$  (Fig. 2). During motion, the slide was guided by a rail located on the slope/tank axis, using low friction wheels, and slid a short distance (4 mm) above the plane incline.

Measured data includes *slide kinematics*, obtained from slide acceleration measured using a micro-accelerometer embedded within the slide, as well as the time of passage of the slide through three electro-magnetical gates (see, Enet and Grilli, 2007, for details), *surface elevation* at up to four capacitance wave gages, and wave runup at the tank axis. Each experiment was repeated twice and both raw and averaged data is provided for each case.

## **2 Experimental Setup and slide geometry**

The laboratory experiments were performed in the University of Rhode Island (URI) wave tank, of width 3.6 m, length 30 m and depth 1.8 m. To do so, a plane aluminum slope of angle  $\theta = 15^\circ$  was built in the middle of the tank (Fig. 1). Water depth was set to  $h_o = 1.5$  m in all experiments (Fig. 2).

The underwater slide was fabricated in aluminum, with a Gaussian shape geometry (Fig. 3) of length  $b = 0.395$  m, width  $w = 0.680$  m, and thickness  $T = 0.082$  m, defined as,



Figure 1: Experimental set-up for Enet and Grilli's (2007) underwater landslide experiments.

$$\zeta = \frac{T}{1-\epsilon} \{ \operatorname{sech}(k_b \xi) \operatorname{sech}(k_w \eta) - \epsilon \} \quad (1)$$

with,

$$k_b = \frac{2C}{b} \quad (2)$$

$$k_w = \frac{2C}{w} \quad (3)$$

$$C = \operatorname{acosh}\left(\frac{1}{\epsilon}\right) \quad (4)$$

With these definitions, the external slide volume was obtained by integrating slide geometry as,

$$V_b = b w T \left( \frac{f^2 - \epsilon}{1 - \epsilon} \right) \quad \text{with} \quad f = \frac{2}{C} \operatorname{atan} \sqrt{\frac{1 - \epsilon}{1 + \epsilon}} \quad (5)$$

This volume was precisely measured after fabricating the slide, to  $V_b = 6.57 \times 10^{-3} \text{ m}^3$ , which using the above equations and slide geometric data yields,  $\epsilon = 0.717$ .

For each submergence depth  $d$ , the slide initial abscissa  $x_i$  and the abscissa of the slide point of maximum thickness  $x_0$  are defined and related as,

$$x_0 = x_i + T' \sin \theta = \frac{d}{\tan \theta} + \frac{T'}{\sin \theta} \quad (6)$$

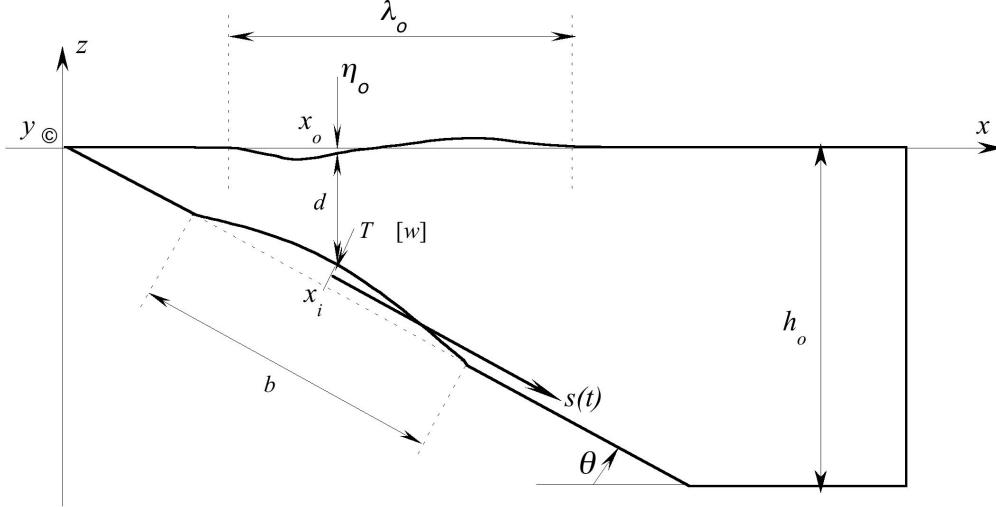


Figure 2: Vertical cross section for underwater landslide experiments, where  $(b, w, T)$  denote slide length, width and thickness,  $d$  is initial submergence depth.  $x = x_i$  is initial slide abscissa on slope, and  $x_o$  is the abscissa of the first wave gage located at the location of slide maximum thickness. Finally,  $\eta_0$  is defined as the maximum initial surface depression measured at  $x_o$ .

where  $T' = T + 0.004$  (in m), since in experiments the landslide was sliding at 4 mm above the slope, in order to achieve negligible friction.

The slide had a central cavity housing the micro-accelerometer, which partly filled with water. Taking this into consideration, slide mass was measured at  $M_b = \rho_b V_b = 16.00$  kg and its bulk density (based on measured volume) was  $\rho_b = 2,435$  kg/m<sup>3</sup>.

### 3 Slide kinematics

According to classical mechanics, the slide model center of mass motion  $s(t)$  (Fig. 2), parallel to the slope, is expressed by balancing inertia, gravity, buoyancy, Coulomb friction, hydrodynamic friction and drag forces as (Enet and Grilli, 2007),

$$(M_b + \Delta M_b)\ddot{s} = (M_b - \rho_w V_b)(\sin \theta - C_n \cos \theta)g - \frac{1}{2}\rho_w(C_F A_w + C_D A_b)\dot{s}^2 \quad (7)$$

(upper dots denote time derivatives) with  $\rho_w$  the water density,  $g$  the gravitational acceleration,  $(C_F, C_D)$  the slide skin friction and form drag coefficients,  $C_n = \tan \psi$  the basal Coulomb friction coefficient,  $\Delta M_b$  the slide added mass,  $A_w$  the slide wetted surface area, and  $A_b$  the slide main cross-sectional area perpendicular to the direction of motion. Based

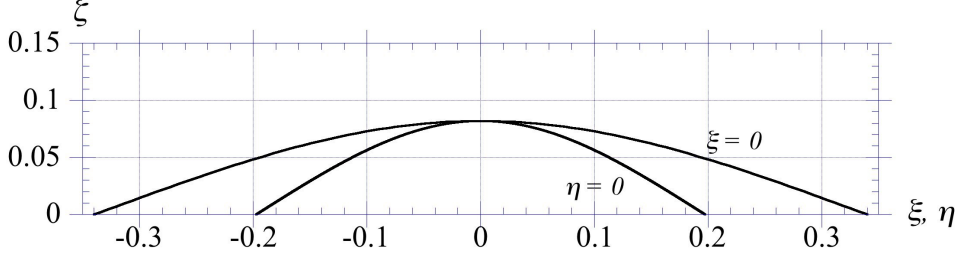


Figure 3: Vertical cross sections in landslide model geometry defined by Eq. (1) (dimensions are in meters).

on this, the added mass coefficient and global drag coefficient of the complete system are defined as,  $C_m = \Delta M_b / \rho_w V_b$  and  $C_d = C_F A_w / A_b + C_D$ .

Hence, the slide equation of motion simplifies to,

$$(\gamma + C_m)\ddot{s} = (\gamma - 1)(\sin \theta - C_n \cos \theta)g - \frac{1}{2}C_d \frac{A_b}{V_b} \dot{s}^2 \quad (8)$$

where  $\gamma = \rho_b / \rho_w$  and, based slide on geometry,

$$A_b = Tw \left( \frac{f - \epsilon}{1 - \epsilon} \right) \quad (9)$$

This equation can be solved analytically, assuming  $s = 0$ ,  $\dot{s} = 0$ , and  $\ddot{s}(0) = a_0$ , for  $t = 0$ , and  $\dot{s} \simeq u_t$  and  $\ddot{s} \simeq 0$ , for  $t \rightarrow \infty$ , to yield,

$$s(t) = s_0 \log(\cosh \frac{t}{t_0}) \quad (10)$$

$$\dot{s} = u_t \tanh(\frac{t}{t_0}) \quad (11)$$

$$\ddot{s} = a_0 \cosh^{-2}(\frac{t}{t_0}) \quad (12)$$

with,

$$t_0 = \frac{u_t}{a_0} \quad (13)$$

$$s_0 = \frac{u_t^2}{a_0} \quad (14)$$

$$(15)$$

the slide characteristic time and distance of center of mass motion. With these definitions, the landslide initial acceleration and terminal velocity read,

$$a_0 = g \sin \theta \left( 1 - \frac{\tan \psi}{\tan \theta} \right) \left( \frac{\gamma - 1}{\gamma + C_m} \right) \quad (16)$$

$$u_t = \sqrt{gd} \sqrt{\frac{b \sin \theta}{d} \left(1 - \frac{\tan \psi}{\tan \theta}\right) \frac{(\gamma - 1)}{C_d} \frac{2(f^2 - \epsilon)}{f - \epsilon}} \quad (17)$$

which can both be calculated based on slide geometric data and density ratio  $\gamma$ , provided the hydrodynamic coefficients ( $C_m, C_d$ ) are known, with for  $\epsilon = 0.717$ ,  $C = 0.8616$  and  $f = 0.8952$ .

For each experiment, these hydrodynamic coefficients were calculated as least-square fits, by applying the above equations to the measured slide kinematics, expressed as a composite of center of mass acceleration  $\ddot{s}(t)$  and time of passage at the known position of the 3 electro-mechanical gates (see Enet and Grilli, 2007, for details). Results are given later.

## 4 Experimental parameters and measured data

Experiments were performed for different initial submergence depths  $d$ , which are listed in Table 1, together with values of related slide parameters and some measured tsunami waves characteristics. [Note the slight difference between the actual measured value of  $x_0$  and the theoretical value, due to experimental variance.]

$d$ (mm)	61	80	100	120	140	149	189
$x_0$ (mm) (measured)	551	617	696	763	846	877	1017
$x_0$ (mm) (theoretical)	560	630	705	780	854	888	1037
$\eta_0$ (mm)	13.0	9.2	7.8	5.1	4.4	4.2	3.1
$R_u$ (mm)	6.2	5.7	4.4	3.4	2.3	2.7	2.0
$C_m$	0.601	0.576	0.627	0.679	0.761	0.601	0.576
$C_d$	0.473	0.509	0.367	0.332	0.302	0.364	0.353
$a_0$ (m/s <sup>2</sup> )	1.20	1.21	1.19	1.17	1.14	1.20	1.21
$u_t$ (m/s)	1.70	1.64	1.93	2.03	2.13	1.94	1.97
$t_0$ (s)	1.42	1.36	1.62	1.74	1.87	1.62	1.63
$s_0$ (m)	2.408	2.223	3.130	3.522	3.980	3.136	3.207

Table 1: Measured and curve-fitted slide and wave parameters for various initial submergence depths

Four capacitance wave gages were mounted in the tank to measure surface elevation during landslide motion (Fig. 4). Gage 1 was moved between experiment to always be

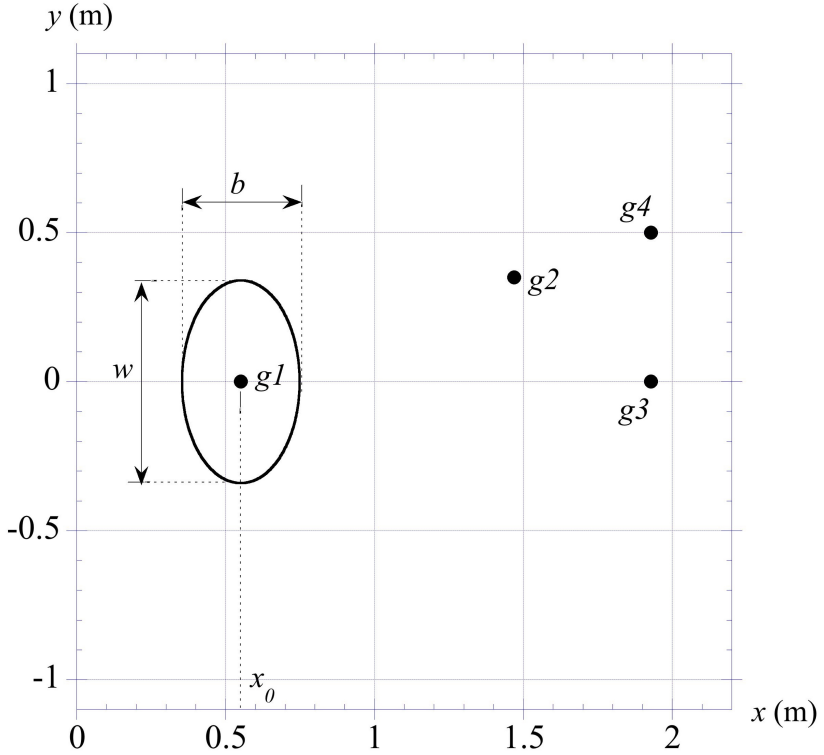


Figure 4: Landslide and gage locations (Table 2). Figure is drawn for case  $d = 61$  mm.

located at  $(x = x_0, y = 0)$ . Coordinates of the other gage locations in the horizontal plane  $(x, y)$  are given in Table 2.

$(mm)$	gage 1 ( $g1$ )	gage 2 ( $g2$ )	gage 3 ( $g3$ )	gage 4 ( $g4$ )
$(x, y)$	$(x_0, 0)$	(1469,350)	(1929,0)	(1929,500)
$(r, \phi)$	$(x_0, 0)$	(1510,13.5°)	(1929,0)	(1992,14.3°)

Table 2: Wave Gauges Locations. The second line is polar coordinates.

Because raw measurements of slide kinematics were significantly processed in order to curve-fit the hydrodynamic coefficients corresponding to each experiment (i.e., average of 2 replicates), these are not provided here. Instead, in Table 1, we provide the curve fitted values of  $C_m$ ,  $C_d$ ,  $a_0$ ,  $u_t$ ,  $s_0$  and  $t_0$ , based on the average of the measured kinematics for each experiment.

Then, in data file *kinematics* (.txt or .xls), we provide values of  $(t, s(t))$ , recalculated for each average experiment, using Eq. (10) and the values of  $s_0$  and  $t_0$  listed in Table 1 (calculated using Eqs. (13,14) and the other data in the table). Finally, Fig. 5 shows a plot of

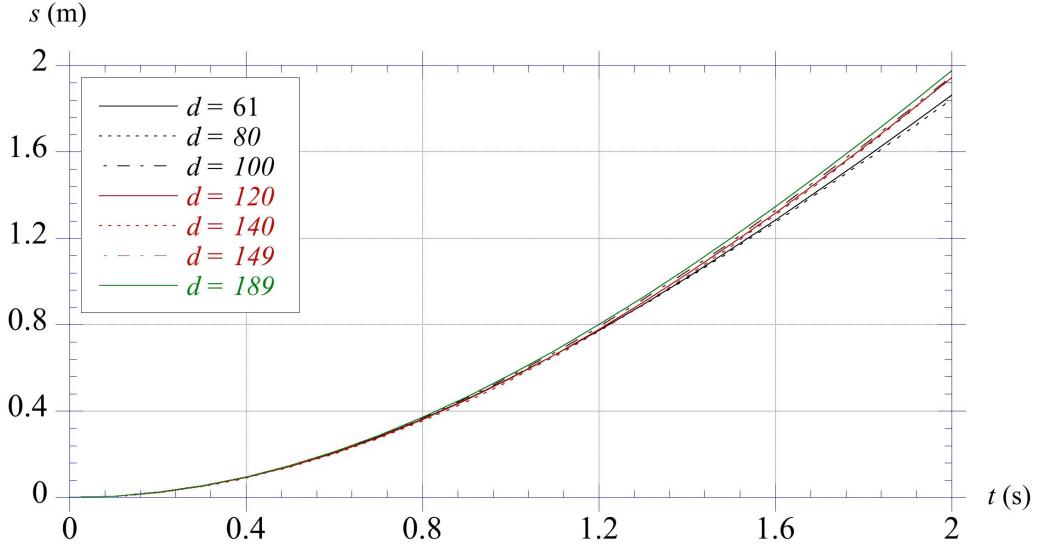


Figure 5: Experimental slide kinematics, as a function of initial submergence depth  $d$ , calculated with Eqs. (10, 13, 14) using average experimentally fitted values of  $t_0$  and  $s_0$  from Table 1.

the same data as given in the file, for each experiment. We see that the average kinematics is nearly identical for all tests, up to 1.2 s or so. For later times, small differences in kinematics arise due to experimental variability of the slide motion down the slope.

Regarding tsunami wave elevations, Table 1, lists for each case the measured characteristic tsunami amplitude  $\eta_0$  (maximum depression at gage 1) and maximum runup on the tank axis  $R_u$ . Note, these small runup values were measured using a small digital camera directly viewing the waterline motion over a graduated scale. One should be cautioned that runup values might have been slightly affected by effects of the slide guiding rail.

Seven data files are provided (in both .txt and .xls), which contain, for each of the 7 initial submergence depths ( $d = 61, 80, 100, 120, 140, 149, 189$  mm), all time series of surface elevation measured at up to the 4 gages (in mm), listed ( $g1, g2, g3, g4$ ). In each file, when available, results are provided for each of two experimental replicates (or runs, marked as  $r1$  or  $r2$ ), done for the same initial slide parameters, and for their average (marked as  $ave$ ). In some of the tests, data was missing for one of the runs and/or for one of the gages. In the latter case, this is identified in the name tag given each file. For instance, "d61g1234" (.txt or .xls), indicates that these are results for depth  $d = 61$  mm and gages 1, 2, 3, and 4. Finally, data files are all provided as tab-delimited text files (with one line of title to skip) and excel spreadsheets. Fig. 6 shows all surface elevations available at gages for each experiment.

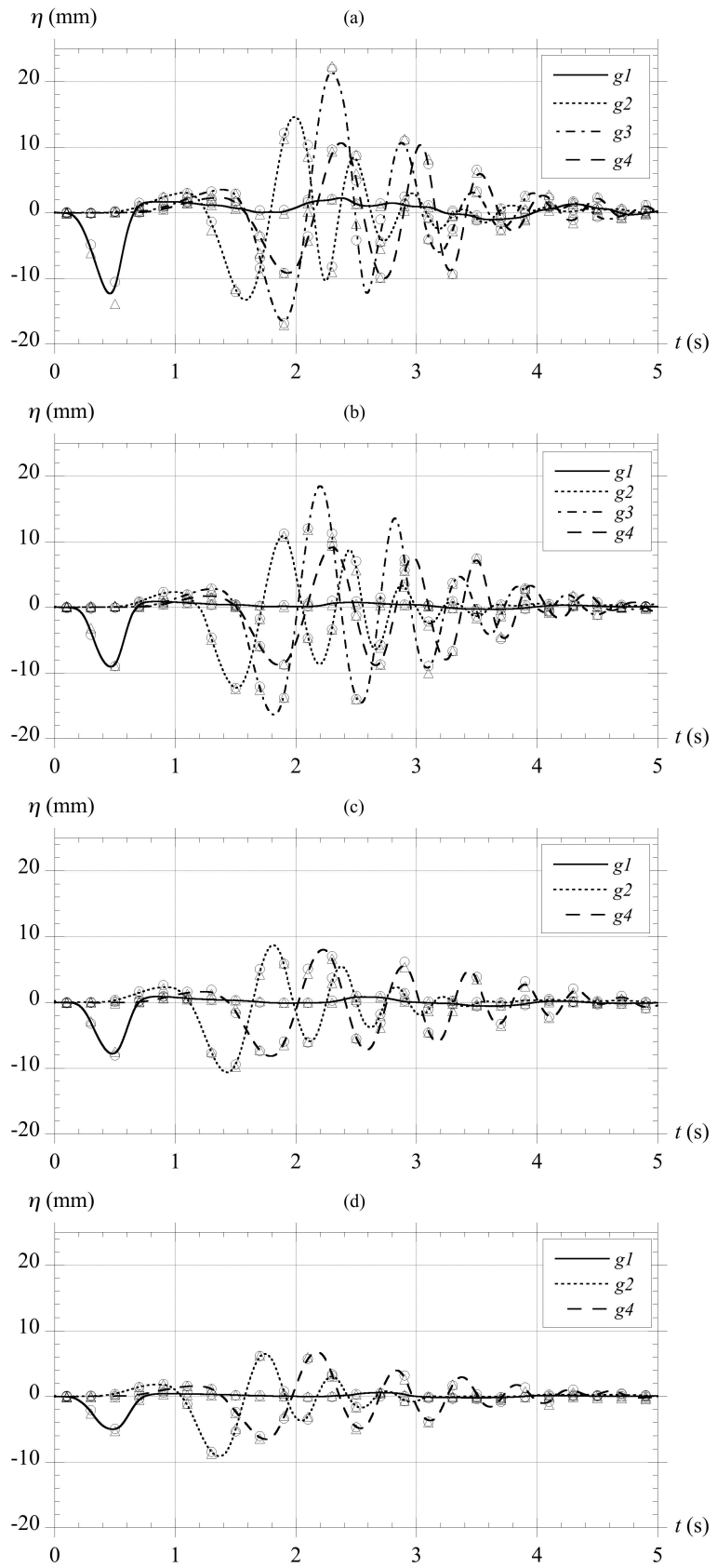
Solid curves are plotted for the average of 2 replicates and symbols denote partial raw data for each replicate.

## 5 Numerical simulations

Simulations of some of these experiments using a three-dimensional Fully Nonlinear Potential Flow model (based on a higher-order boundary element method; Grilli et al., 2002) were reported by Enet et al. (2003, 2005) and Grilli et al. (2010). Simulations of some of these experiments based on a high-order Boussinesq model were reported by Fuhrman and Madsen (2009). Finally, similar simulations were reported using a shock-capturing (sigma-level) non-hydrostatic model (Ma et al., 2011).

## 6 References

- Enet, F, Grilli, S.T. and Watts, P. (2003). Laboratory Experiments for Tsunamis Generated by Underwater Landslides: Comparison with Numerical Modeling. In *Proc. 13th Offshore and Polar Engng. Conf.* (ISOPE03, Honolulu, USA, May 2003), 372-379.
- Enet F. and Grilli S.T. (2005). Tsunami Landslide Generation: Modelling and Experiments. In *Proc. 5th Intl. on Ocean Wave Measurement and Analysis* (WAVES 2005, Madrid, Spain, July 2005), IAHR Publication, paper 88, 10 pps.
- Enet, F. and Grilli, S.T. (2007). Experimental Study of Tsunami Generation by Three-dimensional Rigid Underwater Landslides. *J. Waterway Port Coastal and Ocean Engng.*, **133**(6), 442-454.
- Fuhrman D.R. and P.A. Madsen (2009). Tsunami generation, propagation, and run-up with a high-order Boussinesq model. *Coastal Engineering*, **56**, 747-758.
- Grilli, S.T., Vogelmann, S. and Watts, P. (2002). Development of a 3D Numerical Wave Tank for modeling tsunami generation by underwater landslides. *Engineering Analysis with Boundary Elements*, **26**(4), 301-313.
- Grilli, S.T., Dias, F., Guyenne, P., Fochesato, C. and F. Enet (2010). Progress In Fully Nonlinear Potential Flow Modeling Of 3D Extreme Ocean Waves. Chapter 3 in *Advances in Numerical Simulation of Nonlinear Water Waves* (ISBN: 978-981-283-649-6, edited by Q.W. Ma) (Vol. 11 in Series in Advances in Coastal and Ocean Engineering). World Scientific Publishing Co. Pte. Ltd., pps. 75-128.
- Ma, G., Shi, F. and J.T. Kirby (2011). Shock-capturing Non-hydrostatic Model for Nearshore Wave Processes. *Ocean Modeling* (submitted).



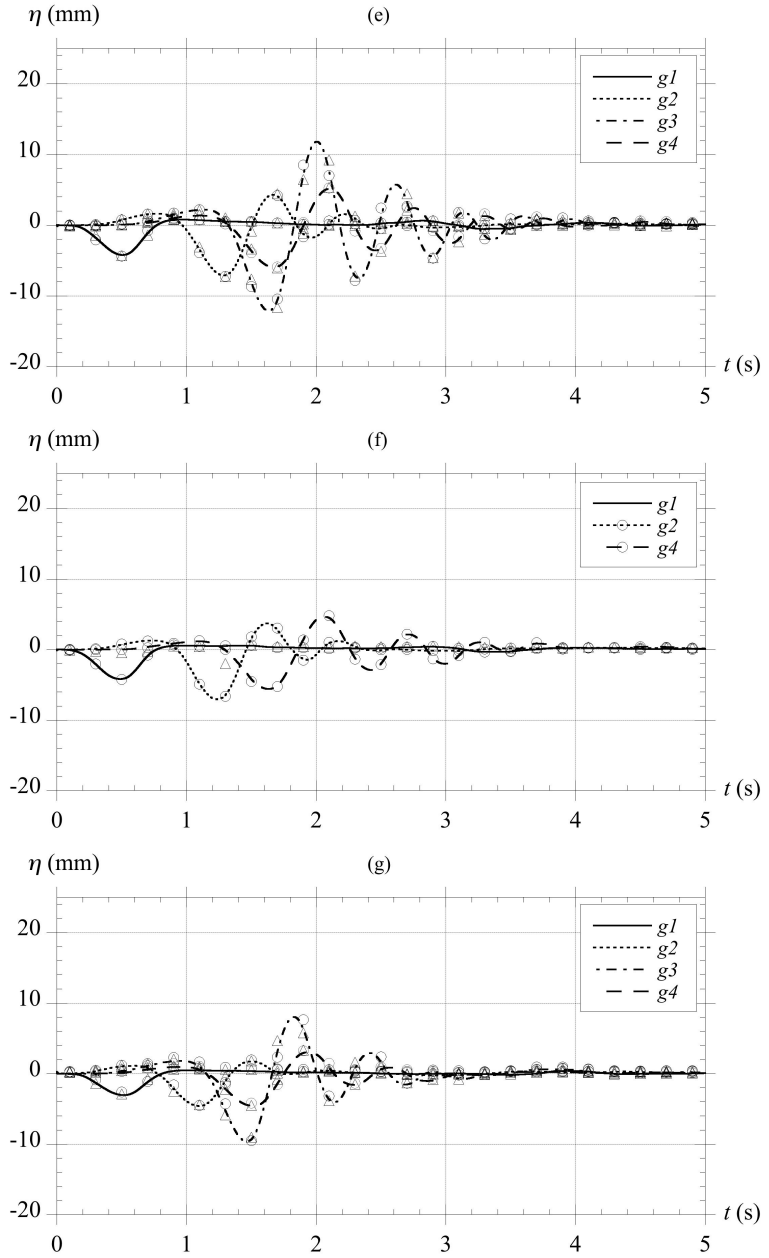


Figure 6: Surface elevation measured at gages ( $g1, g2, g3, g4$ ) in underwatwer slide experiments. Symbols ( $\circ$ ) and ( $\triangle$ ) denote experimental runs  $r1$  and  $r2$ , respectively (1% of data points are shown), and lines denote their average. Initial slide submergence is as listed in Table 1,  $d =$  (a) 61, (b) 80, (c) 100, (d) 120, (e) 140, (f) 149, (g) 189 mm (see Fig. 2).